Si Binding and Nucleation on Si(100)

Peter J. Bedrossian
L-350, Lawrence Livermore National Laboratory, Livermore, California 94550
(Received 16 November 1994)

Si adatoms deposited on Si(100)-(2 × 1) below 200 °C assume metastable binding configurations, each distinct from the dimer string topology ordinarily observed following deposition at higher temperatures. Isolated ad-dimers which nucleate predominantly on substrate dimer rows at room temperature do not constitute the precursors for dimer strings. Instead, they transform upon annealing at ≈120 °C to metastable, dimerized lines assembled end to end, parallel to the substrate's dimer bonds.

PACS numbers: 68.55.Jk, 68.35.Bs

The need to control dopant incorporation and diffusion in epitaxial Si has contributed to recent efforts to develop silicon molecular beam epitaxy near room temperature [1–4]. While it has already been recognized that Si deposited on Si(100)-(2 × 1) near room temperature adopts metastable adsorbate structures, the associated atomic topologies have not yet been identified [5]. It is therefore critical to characterize the configurations and stability of those adatom structures which mediate the evolution of the morphology of Si(100) during homoepitaxial growth near room temperature.

The anisotropic character of the growth of Si(100)-(2 × 1), of atomic diffusion on that surface, and of the organization of adatoms into dimerized strings under epitaxy well above room temperature, have been established experimentally [6–12]. Anisotropic growth has also been characterized with statistical models [13–15]. The experimentally observed diffusional anisotropy on Si(100)-(2 × 1), favoring motion of Si adatoms parallel to the substrate dimer rows [9–11], has been reproduced in molecular dynamics and Monte Carlo calculations [16–18], which have also provided insight into the incorporation of diffusing adatoms into dimer strings on that surface [19–26]. While first-principles methods [27,28] and molecular dynamics [29] have been used to compare the energetics of single atom and dimer adsorption sites on Si(100), concerted atomic motion has been shown in the empirical studies to enable particular diffusion paths, and therefore novel atomic configurations, which would not be accessible by single-atom motion alone.

Most of these previous investigations have addressed the formation and growth of dimer strings as occur following deposition well above room temperature. Here we present a hierarchy of metastable adsorption configurations which occur near room temperature. Because these structures dominate Si/Si(100) growth at those temperatures, room-temperature growth has a qualitatively different character from epitaxy at higher temperatures. The description of growth near room temperature must therefore address the kinetics of formation and transformation of those observed configurations.

The experiments employed an ultrahigh vacuum (UHV) chamber with base pressure below 10^{-10} torr. The Si(100) sample was cleaned initially by heating to 1250 °C, after which it yielded a strong (2 × 1) periodicity in low-energy electron diffraction (LEED) and tunneling microscopy (STM). Si was deposited from a thoroughly degassed, heated wafer at ≈8×10^{-4} monolayers per second (ML/s), during which the chamber pressure remained below 2×10^{-10} torr. The sample could be heated resistively during or after deposition, and sample temperatures were calibrated with a type *C* thermocouple. After deposition and equilibration to room temperature, the sample was transferred *in situ* to a commercial STM (Omicron Associates) for imaging. All images were acquired with constant tip-sample current, with greater tip-sample separation represented by a brighter shade of grey.

Figure 1 presents a pair of STM images of a region of a Si(100) surface following deposition of ≈0.004 ML of Si with the substrate at room temperature. As described previously, the bright, diagonal bands on the substrate in the filled-state image, acquired with the sample biased −1.3 V with respect to the STM tip, represent individual dimer rows, which appear in the corresponding empty-state image as darkened bands [30]. Because the empty-state image is sensitive to dangling-bond orbitals associated with individual atoms, it enables the identification of individual dimerized atoms, which might appear as a single entity in a filled-state image. A short dimer row at the lower right of the image, labeled *Q*, is therefore identified by the distinctive appearance of two lobes in the empty-state image. Although such rows do appear even at room temperature, the surface is dominated by isolated structures, labeled *R*, sitting atop the substrate's dimer rows. Once again, the sensitivity of the empty-state image to individual atoms affords the resolution of the identified structures into two atoms; those indicated are dimerized parallel to the substrate's dimer rows.

Individual Si dimers in such a configuration have been identified previously [11]. Although the *R* pairs in Fig. 1 assume the orientation consistent with that of a layer which grows epitaxially, they do not aggregate directly into *Q*-type structures with annealing. Furthermore, the *R*-type structures themselves are unstable to exchange between two mutually orthogonal orientations, and are therefore analogous to a metastable configuration of Sb

 0031-9007/95/74(18)/3648(4)$06.00

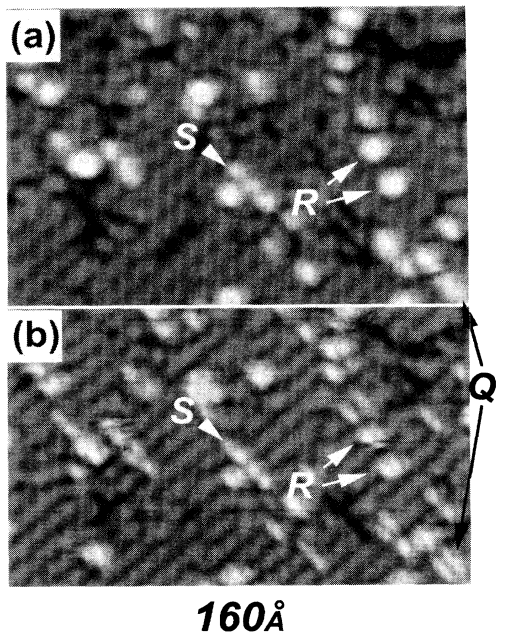

FIG. 1. Pair of STM images showing adsorbate structures on Si(100) following room-temperature deposition of ≈0.004 ML Si. The structures labeled Q, R, and S are known conventially as dimer rows, single dimers, and "diluted" dimers, respectively. (a) Filled states, with sample bias = −1.3 V; (b) empty states with sample bias = +1.3 V. The tunnel current is 0.2 nA.

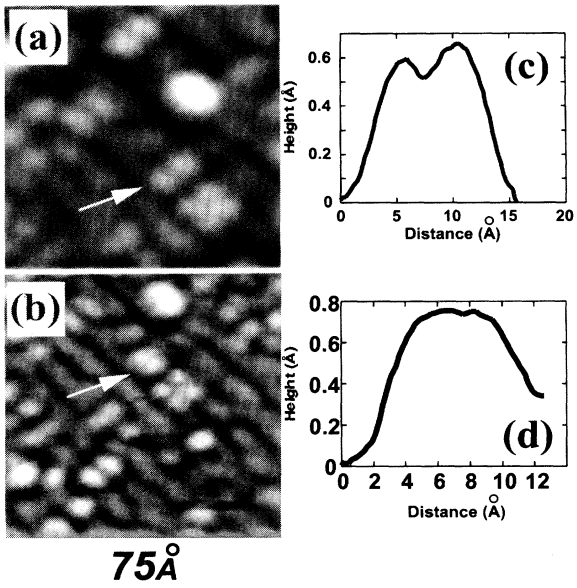

FIG. 2. Empty-state STM images acquired $\frac{1}{2}$ min apart, showing the exchange of a single adsorbed dimer, indicated by an arrow, first (a) parallel, and then (b) perpendicular to the dimer bonds in the substrate. Thermal drift results in the translation of the features in (b) relative to (a). Line cuts (c) and (d) to the right of each image plot the variation in tip height along the direction of the dimer bond and demonstrate the resolution of the dimer into two distinct atoms. The zero of each dimension is arbitrary. Sample bias = +1.4 V, 1 nA.

dimers, whose binding configurations and kinetics have been discussed thoroughly [31–34].

Figure 2 presents two representative empty-state images showing the reversible interchange in orientation of such a pair at room temperature, together with line traces along the dimer bonds of each indicated pair. Empty-state images are shown to enhance the resolution of the individual adatoms which constitute the ad-dimers. The appearance of the two orientations in the STM images is consistent with their recently predicted near degeneracy [28,29]. While the STM tip itself may still facilitate the observed exchange, the conversion rate observed here for Si dimers appeared independent of the tip-sample bias, from 1 to 2.5 V, in contrast to observations reported for Sb dimers. Moreover, the isolated dimers remained parallel to the substrate dimer rows in 85% of the images at two different scan rates, 4 s/frame and 8 s/frame. The detailed structural description of the dimer orientation change may involve pathways which include atomic exchange with the substrate, which would not be distinguished by the experimental approach used here, but might be explored theoretically.

Figure 1 contains a third structure, labeled S, which in the filled-state image consists of three bright spots, each lying in a trough between substrate dimer rows, and ordered in a line perpendicular to those rows. Such structures were previously identified as "diluted dimers" because their appearance in the filled-state image suggested a dimer row containing only that sublattice of its constituent dimers which would lie in troughs between substrate rows. However, the empty-state image of the same structure does not display the two-lobed topology of the Q structure in the same image; therefore, the S structure, in contrast to the Q, is not composed of dimers oriented perpendicular to the substrate dimer bonds.

Annealing a surface such as that in Fig. 1 for 2 min at 120 ± 40 °C results in a rearrangement leaving the S structure identified in Fig. 1 as the prevalent adsorbate configuration. A similar surface was previously associated with Si deposition below 350 °C [5]. Comparison of the filled- and empty-state images of one of these structures in Fig. 3 indicates that each constituent bright spot within a trough in the filled-state image appears as two distinct atoms in the empty-state image, according to Fig. 4. If their apparent melding in the filled-state image indicates dimerization, then the dimer bonds in this structure form parallel to those of the substrate. In contrast, the dimer bonds in the more stable Q structure in Fig. 1 lie perpendicular to those of the substrate.

The irregular buckling of substrate dimer rows in Fig. 3 gives that substrate a high degree of disorder relative to the starting surface, clean Si(100). It has been shown that the presence of defects on Si(100) can give rise to such long-range, buckled regions on the surrounding substrate [35], and that substrate defects affect the formation and

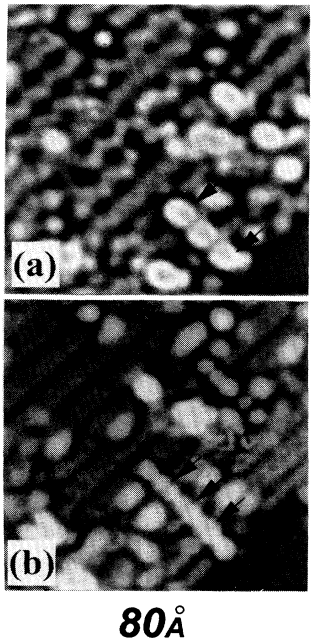

FIG. 3. Pair of STM images showing a row of dimers arranged end to end, parallel to the substrate's dimer bonds. In both (a) the filled-state (sample bias = −1.1 V) and (b) empty-state (sample bias = +1.1 V) images, three arrows point to the constituent dimers lying in the troughs between substrate dimer rows. The tunnel current is 0.2 nA.

stability of ad-dimer rows [12]. The stability of nuclei and clusters on Si(100) as occur in Figs. 1–3 may therefore be related to long-range interactions involving the clusters and their environment.

Additional atoms often appear at one or both ends of the *S* structures in empty-state images, as in Fig. 3(b). Their position is labeled *T* in Fig. 4. In these cases, we observe an apparent absence in the filled-state image of at least one of the substrate dimers at the end of the adsorbate row, equivalent to the *A* dimer in Fig. 4. Although we do not resolve the details of the rebonding of the substrate atoms in the *A* dimer of Fig. 4, the role of their bonding topology in the kinetic path for atom incorporation at the ends of the *S* structures undoubtedly underlies the growth mechanism of those structures.

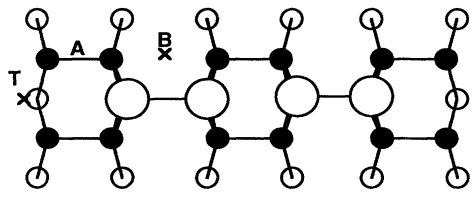

FIG. 4. Schematic diagram of the structure labeled *S* in Fig. 1 and shown in detail in Fig. 3. Large open circles represent adatoms, filled circles represent atoms in the substrate surface layer, and small open circles indicate atoms in the next layer down. The labeled sites are identified in the text. The substrate dimer bonds are drawn for orientation only and may not represent a real bonding topology after adsorption.

The ordering of adatoms into metastable lines of dimers arranged end to end, called *S* structures above, does not appear to have been anticipated by either the first-principles or empirical models cited above. A first-principles calculation did identify the sites labeled *T* in Fig. 4 as the most stable binding sites for a single adatom [27], and one empirical calculation identified that site as slightly higher in energy than the position labeled *B* for single-adatom adsorption [16]. However, neither calculation predicted a propensity for the formation of one-dimensional, ordered structures atop those sites, identified as *S* structures above. Another first-principles calculation [28] and an empirical calculation [29] found a near degeneracy in energy for the two switching ad-dimer configurations in Fig. 2; however, the former predicted as the lower-energy configuration that which is observed less frequently [Fig. 2(a)]. Once again, the formation, growth, and decomposition of this structure may involve complicated pathways and possible long-range, interatomic forces which might influence nucleation, but which have not yet been incorporated into models of growth on this surface.

Finally, the hierarchy of dominant, metastable configurations of Si nuclei presented here is undoubtedly not an exhaustive taxonomy. For example, Fig. 2 shows a four-atom cluster beneath the rotating dimer. The existence of such clusters was proposed previously [28], and further work might reveal the relative stabilities of various cluster topologies.

We identified a hierarchy of metastable bonding topologies of Si adatoms occurring on Si(100) following deposition near room temperature, each distinct from the familiar, dimerized (2 × 1) lattice observed following deposition at higher temperatures. Modeling of growth of that surface near room temperature, which has not yet demonstrated kinetic pathways to the formation of these structures, may need to incorporate more complicated trajectories, possibly involving concerted atomic motion, and to address not only the total energies of individual adatoms or ad-dimers but also those of extended structures and their interaction with the surrounding substrate.

The author is especially grateful to Z. Zhang for extensive discussions which stimulated these experiments and for his encouragement. This work was performed under the auspices of the U.S. Department of Energy at Lawrence Livermore National Laboratory under Contract No. W-7405-Eng-48.

[1] D. Eaglesham, H.-J. Gossman, and M. Cerullo, Phys. Rev. Lett. **65**, 1227 (1990).
[2] H.-J. Gossman, E. Schubert, D. Eaglesham, and M. Cerullo, Appl. Phys. Lett. **57**, 2440 (1990).
[3] B. Weir *et al.*, Appl. Phys. Lett. **59**, 204 (1991).
[4] M. V. R. Murty, H. Atwater, A. Kellock, and J. Baglin, App. Phys. Lett. **62**, 2566 (1993).
[5] Y.-W. Mo *et al.*, J. Vac. Sci. Technol. A **8**, 201 (1990).

[6] R. Hamers, U. Köhler, and J. Demuth, Ultramicroscopy **31**, 10 (1989).
[7] A. Hoeven *et al.,* Phys. Rev. Lett. **63**, 1830 (1989).
[8] Y.-W. Mo *et al.,* Phys. Rev. Lett. **63**, 2393 (1989).
[9] Y.-W. Mo, J. Kleiner, M. Webb, and M. Lagally, Phys. Rev. Lett. **66**, 1998 (1991).
[10] Y.-W. Mo and M. Lagally, Surf. Sci. **248**, 313 (1991).
[11] Y.-W. Mo, J. Kleiner, M. Webb, and M. Lagally, Surf. Sci. **268**, 275 (1992).
[12] P. Bedrossian and E. Kaxiras, Phys. Rev. Lett. **70**, 2589–2592 (1993).
[13] J. Y. Tsao, E. Chason, U. Köhler, and R. Hamers, Phys. Rev. B **40**, 11 951 (1989).
[14] S. Clarke, M. Wilby, and D. Vvedensky, Surf. Sci. **255**, 91 (1991).
[15] M. Wilby, M. Ricketts, S. Clarke, and D. Vvedensky, J. Cryst. Growth **111**, 864 (1991).
[16] J. Wang and A. Rockett, Phys. Rev. B **43**, 12 571 (1991).
[17] Y. Lu, Z. Zhang, and H. Metiu, Surf. Sci. **257**, 199 (1991).
[18] Z. Zhang, Y. Lu, and H. Metiu, Surf. Sci. Lett. **248**, L250 (1991).
[19] D. Srivastava and B. Garrison, J. Vac. Sci. Technol. A **8**, 3506 (1990).
[20] Z. Zhang, Y. Lu, and H. Metiu, Surf. Sci. Lett. **255**, L543–L549 (1991).
[21] D. Srivastava and B. Garrison, J. Chem. Phys. **95**, 6885 (1991).
[22] Z. Zhang and H. Metiu, Surf. Sci. **245**, 353 (1991).
[23] Z. Zhang and H. Metiu, Surf. Sci. Lett. **292**, L781 (1993).
[24] D. Srivastava and B. Garrison, Phys. Rev. B **47**, 4464 (1993).
[25] A. Rockett, Surf. Sci. **312**, 201 (1994).
[26] Z. Zhang, H. Chen, B. Bolding, and M. Lagally, Phys. Rev. Lett. **71**, 3677 (1993).
[27] G. Brocks, P. Kelly, and R. Car, Phys. Rev. Lett. **66**, 1729 (1991).
[28] G. Brocks, P. Kelly, and R. Car, Surf. Sci. **269/270**, 860–866 (1992).
[29] Z. Zhang (private communication).
[30] R. Hamers, R. Tromp, and J. Demuth, Phys. Rev. B **34**, 1388 (1986).
[31] Y.-W. Mo, Phys. Rev. Lett. **69**, 3643 (1992).
[32] Y.-W. Mo, Science **261**, 886 (1993).
[33] Y.-W. Mo, Phys. Rev. Lett. **71**, 2923 (1993).
[34] Y.-W. Mo, Phys. Rev. B **48**, 17 233 (1993).
[35] R. Wolkow, Phys. Rev. Lett. **68**, 2636 (1992).

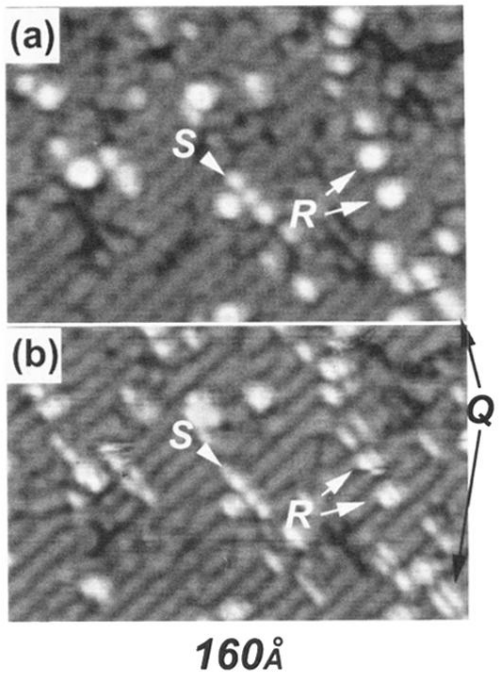

FIG. 1. Pair of STM images showing adsorbate structures on Si(100) following room-temperature deposition of ≈0.004 ML Si. The structures labeled Q, R, and S are known conventially as dimer rows, single dimers, and "diluted" dimers, respectively. (a) Filled states, with sample bias = −1.3 V; (b) empty states with sample bias = +1.3 V. The tunnel current is 0.2 nA.

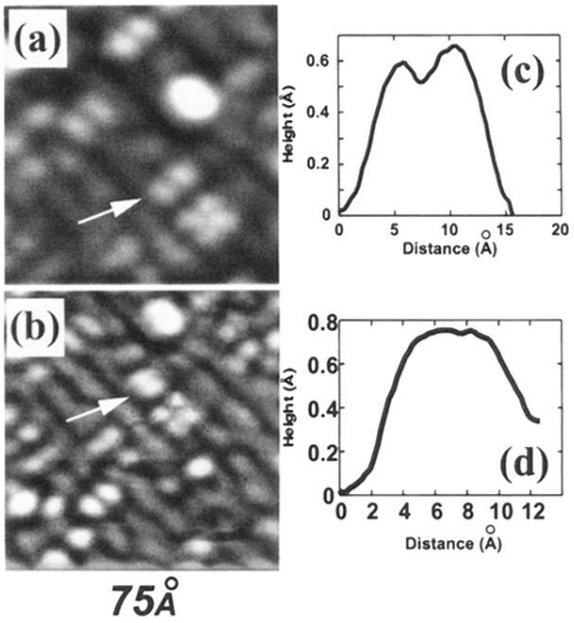

FIG. 2. Empty-state STM images acquired $\frac{1}{2}$ min apart, showing the exchange of a single adsorbed dimer, indicated by an arrow, first (a) parallel, and then (b) perpendicular to the dimer bonds in the substrate. Thermal drift results in the translation of the features in (b) relative to (a). Line cuts (c) and (d) to the right of each image plot the variation in tip height along the direction of the dimer bond and demonstrate the resolution of the dimer into two distinct atoms. The zero of each dimension is arbitrary. Sample bias = +1.4 V, 1 nA.

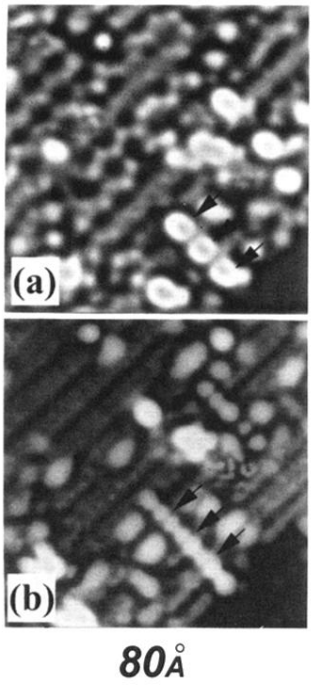

FIG. 3. Pair of STM images showing a row of dimers arranged end to end, parallel to the substrate's dimer bonds. In both (a) the filled-state (sample bias = −1.1 V) and (b) empty-state (sample bias = +1.1 V) images, three arrows point to the constituent dimers lying in the troughs between substrate dimer rows. The tunnel current is 0.2 nA.